Journal of Advanced Marine Engineering and Technology, Vol. 48, No. 1, pp. 9~13, 2024
J. Advanced Marine Engineering and Technology (JAMET)
https://doi.org/10.5916/jamet.2024.48.1.9

ISSN 2234-7925 (Print)
ISSN 2765-4796 (Online)
Original Paper

Recrystallization kinetics and the mechanical properties of low-carbon steel during high-temperature annealing in electric furnace

Sanjaya Kumar Pradhan[1] · Min-Suk Oh[†]

(Received January 26, 2024 ; Revised February 14, 2024 ; Accepted February 27, 2024)

Abstract: In this study, we investigated the microstructures and mechanical properties of annealed cold-rolled low-carbon steels. The specimens were subjected to different annealing temperatures and durations in an electric furnace to investigate their recrystallization phenomena. Recrystallization kinetics were analyzed through microstructural evolution by evaluating various mechanical properties. The results showed that the samples annealed at 700 °C were fully recrystallized with equiaxed grains, whereas equiaxed recrystallized grains began to grow in the samples annealed at 800 °C after 10 min of soaking. Electron backscatter diffraction grain orientation spread maps were used to quantify the percentage of recrystallized grains as a function of annealing temperature and soaking time. The samples annealed at 800 °C with 10 min of soaking exhibited good elongation (approximately 38%) and tensile strength (exceeding 270 MPa).

Keywords: Low-carbon steel, Annealing, Electric furnace, Recrystallization, Mechanical properties

1. Introduction

The shipbuilding industry is constantly working to improve offshore and subsea structures in response to the increasing demand for natural resources, including oil and gas, in underwater environments. Low-carbon steel plates/sheets are widely used in marine industries for major parts of offshore structures that require specific properties such as high strength, high impact toughness, excellent weldability, and corrosion resistance **[1]-[3]**. Grain refinement is a useful strategy for establishing the desired characteristics of the plates **[4]-[8]**. Of the several grain refining methods, cold rolling followed by annealing has been one of the most efficient, effective, and low-cost techniques **[7][8]**. Recrystallization is a common means of investigating the relationship between structure and mechanical properties in carbon steels **[9][10]**.

Recrystallization refers to a high-temperature annealing phenomenon driven by the energy stored in lattice strains and crystal imperfections, such as dislocations, during the deformation process, thereby relaxing the stress in deformed steel when annealed at a particular temperature **[10]-[12]**.

Ferry *et al.* performed continuous annealing of cold-rolled (CR) low- and ultralow-carbon steel **[13]**. Their annealing model, based on the Avrami equation, predicted that the cooling rate and soaking time strongly affect the recrystallization kinetics. Martinez-de-Guerenu *et al.* measured the hardness of recrystallized CR low-carbon steel **[14]**. They found that after annealing at approximately 600 ℃ and 10 s of soaking, the measured Rockwell hardness values decreased as recrystallization initiated. Akbari *et al.* studied the recrystallization kinetics and mechanical properties of low-carbon steel at three different temperatures: room temperature, blue-brittleness, and sub-zero temperature **[15]**. They demonstrated that pre-straining at sub-zero temperature followed by annealing at 600 ℃ enhanced the mechanical properties and recrystallization kinetics better than at room and blue brittleness temperatures. Tian *et al.* reported that ultrafine-grained martensitic low-carbon steel exhibited superior mechanical properties after annealing at 550 ℃ for 30 min **[16]**. However, these studies used conventional heat treatment, which is time- and energy-inefficient, and a major source of CO_2 emissions. Thus, we investigated the recrystallization kinetics of CR low-carbon steel heat-treated in an electric furnace through

† Corresponding Author (ORCID: http://orcid.org/0000-0002-7274-2519): Professor, Division of Advanced Materials Engineering, Graduate School of Integrated Energy AI, Jeonbuk National University, 567, Baekje-daero, Deokjin-gu, Jeonju-si, Jeollabuk-do 54896, Korea, E-mail: misoh@jbnu.ac.kr, Tel: +82-63-270-2297

1 Ph. D. Candidate, Graduate School of Integrated Energy AI, Jeonbuk National University, E-mail: ssanjayapradhan111@gmail.com

microstructural evolution, and measured the mechanical properties of the annealed steel specimens.

2. Experimental Method

Commercial-quality CR low-carbon full hard steel sheets (0.04 C, 0.25 Mn, 0.035 Al, <0.019 P, <0.015 S, Fe balanced in wt. %; 340 × 300 × 1 mm^3) were annealed in an electric furnace at 700 or 800 ℃, soaked for 5 and 10 min, then air cooled. The specimens were cut to 200 × 70 × 1 mm^3 and 10 × 10 × 1 mm^3 for tensile tests and microstructural studies, respectively. Optical microscopy (OM; Leica, DM750), field-emission scanning electron microscopy (FE-SEM; Carl Zeiss, SUPRAA40VP), and scanning electron microscopy/electron backscatter diffraction (SEM-EBSD; JEOL, JIB-4601F) were used for microstructural investigations. Optical microscopy and SEM were conducted on specimens mechanically polished with emery papers (1000–2400 grit size) and finely polished with a 1-μm diamond suspension, followed by chemical etching with 10% nital solution. The specimens were electropolished at 10 V in an acetic acid and perchloric acid solution (80:20) for EBSD characterization. The stress–strain behavior was determined through tensile tests performed at room temperature using a universal testing machine (INSTRON, 8801MTL6258) according to the standard ASTM E8/E8M-22. The Vickers hardness was also measured.

3. Results and Discussion

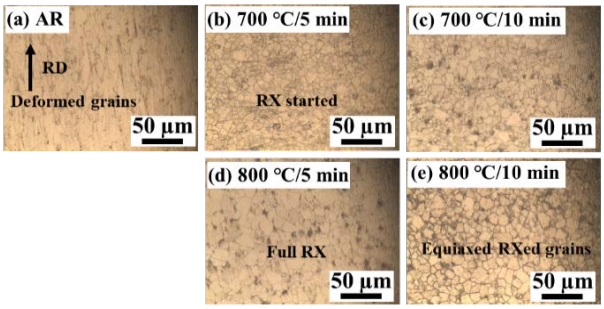

Figure 1: Optical micrographs showing (a) deformed grains elongated along the rolling direction in the AR sample, (b–e) recrystallization phenomena in the annealed samples

Figure 1 shows optical micrographs of the annealed and as-received (AR) samples. The deformed grains are elongated along the rolling direction of the AR sample. After annealing at 700 ℃ with 5 and 10 min of soaking time, as shown in **Figures 1 (b) and (c)**, respectively, static recrystallization initiated with the nucleation of new strain-free grains. In the samples annealed at 800 ℃, equiaxed recrystallized grains were observed **[17][18]**.

Visualization of the microstructures of the samples using FE-SEM, as shown in **Figure 2 (a)-(e)**, revealed similar observations. Heavily deformed grains extend along the rolling direction in the AR sample. Recrystallization was triggered by annealing at 700 ℃, and no microstructural differences were seen in terms of soaking time at this temperature. Full recrystallization occurred in the sample annealed at 800 °C with 5 min of soaking, with equiaxed grains formed throughout. The sample annealed at 800 °C with 10 min of soaking evinced that equiaxed grains started growing when the soaking time increased, as shown in **Figure 2 (e)**. The microstructures of the annealed samples were primarily composed of recrystallized ferrite grains with a small fraction of cementite that tended to nucleate at the grain boundaries **[15][19]**.

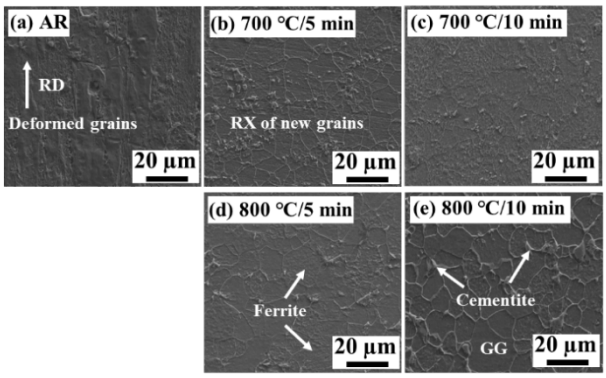

Figure 2: SEM images showing (a) deformed grains elongated along the rolling direction in the AR sample, and (b–e) recrystallization phenomena in the annealed samples; GG refers to grain growth

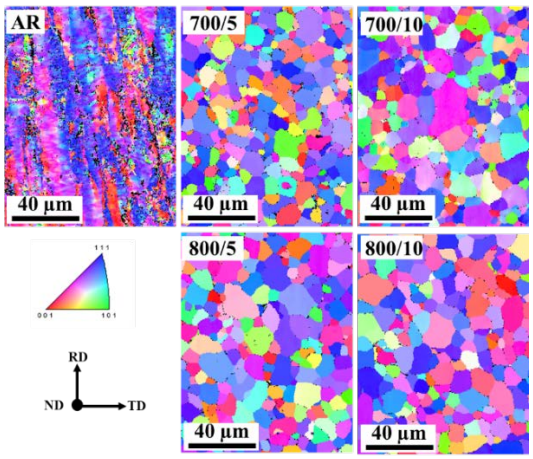

Figure 3: Inverse pole figure maps showing recrystallized ferrite grains oriented along <111> //ND and <110> //ND in annealed samples

Inverse pole figures were obtained to examine the textural evolution of the annealed specimens, which showed recrystallized ferrite grains oriented along <111> // ND and <110> // ND, as shown in **Figure 3 [20]-[22]**. The strong texture indicates that recrystallization occurred after annealing at both temperatures.

The percentages of recrystallized grains formed in the annealed samples are indicated by the grain orientation spread maps shown in **Figure 4**. The percentage of recrystallization is increased by 2–3% with the increase in annealing temperature, from approximately 95–96% at 700 ℃ to 97–98% at 800 ℃. Moreover, the soaking duration has a minimal effect on the recrystallization percentage at both annealing temperatures **[22]**.

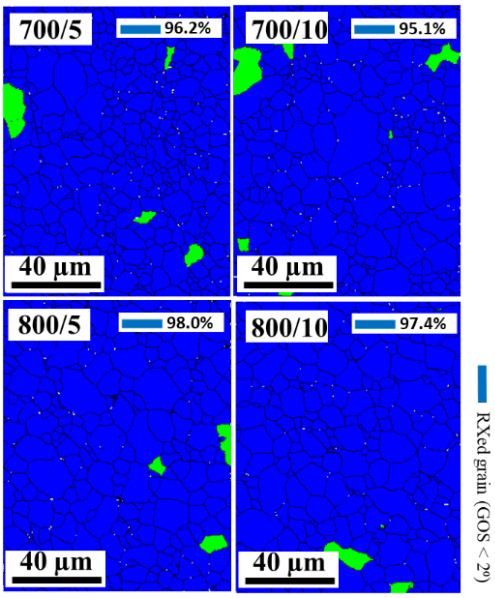

Figure 4: Grain orientation spread (GOS) maps showing the recrystallization percentage in the annealed samples. GOS < 2° are treated as recrystallized grains **[22]**

The average grain size of the annealed samples was measured and it was observed that the average size of the recrystallized grains increased with annealing temperature and soaking time, as shown in **Figure 5**. The average grain size for the specimen annealed at 700 °C and soaked for 5 min was approximately 5 µm, whereas the specimen annealed at 800 °C and soaked for 10 min had the largest grain size, measuring approximately 7 µm. This validated the phenomenon of grain development that occurred throughout the annealing process.

To investigate the effect of heat treatment on the mechanical properties, tensile tests were conducted on all samples. The tensile strength (TS) and strain obtained for each specimen are listed in **Table 1**, and the stress–strain curves are shown in **Figure 6**. The annealing temperature influenced TS: the TS of the annealed samples was nearly three times lower than that of the AR samples. The samples annealed at 800 ℃ exhibited greater elongation and lower TS than those annealed at 700 ℃. Soaking time had negligible effect on the ductility of the annealed specimens: the sample annealed at 800 °C and soaked for 10 min showed 38% elongation, four percentage points more than the sample annealed at 800 °C and soaked for 5 min.

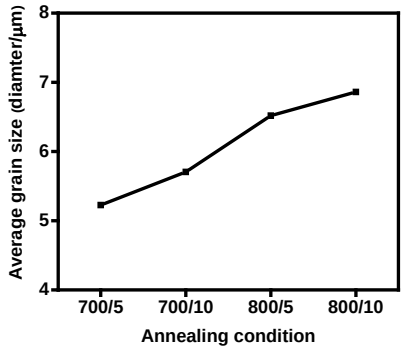

Figure 5: Average grain size plotted against samples' annealing conditions

Table 1: Tensile strength and tensile strain for AR and annealed samples

Samples	**Tensile strength** (MPa)	**Tensile Strain** (%)
AR	830	1
700/10	377	30
800/5	280	34
800/10	275	38

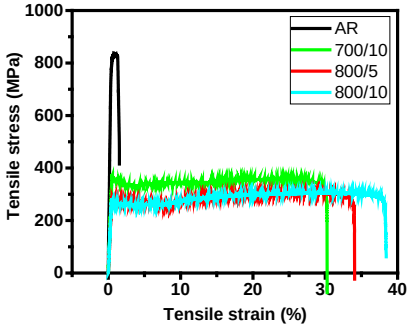

Figure 6: Stress–strain curves obtained for AR and annealed samples

The Vickers hardness of all the specimens was measured as an indicator of recrystallization. **Figure 7** shows the recrystallization fraction and Vickers hardness as functions of the annealing

conditions. As the annealing temperature and duration increased, the hardness decreased, whereas the recrystallization fraction increased proportionally. The increased average grain size in samples annealed at 800 ℃ led to a reduction in hardness compared to those annealed at 700 ℃.

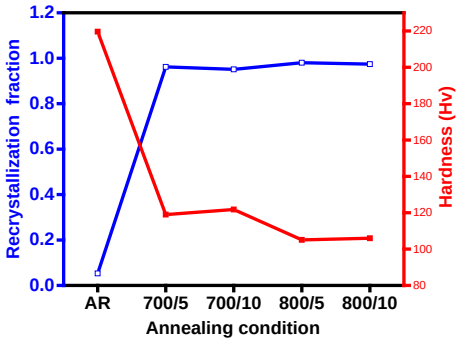

Figure 7: Measured recrystallization fraction and corresponding Vickers hardness values plotted as a function of annealing condition

The progression of recrystallization was examined via microstructural analysis and mechanical property measurements. The tensile strength and hardness of the specimens decreased with increasing annealing temperature and time, suggesting an increase in recrystallization with increased annealing parameters. This trend is further evident in the EBSD map, where the highest proportion of recrystallized grains is observed in the samples annealed at 800 °C.

4. Conclusion

This study analyzed the recrystallization of CR low-carbon steel annealed in an electric furnace at either 700 ℃ or 800 ℃ with 5 or 10 min of soaking. The following conclusions were drawn.

1) OM, SEM, and EBSD showed that annealing at 700 ℃ for 5 min is sufficient to initiate recrystallization.
2) Ferrite grains form after soaking for 10 min at 800 ℃.
3) The sample annealed at 800 °C and soaked for 10 min exhibited an excellent elongation of 38% and approximately 270 MPa tensile strength.

Acknowledgement

The study was supported by a National Research Foundation of Korea (NRF) grant funded by the Korean government (Ministry of Science and ICT) (grant no. 2022R1A2C1008972) and the Ministry of Trade, Industry, and Energy (MOTIE) and the Korea Institute of Energy Technology Evaluation and Planning (KETEP) in 2023 (grant no. RS-2023-00233397).

Author Contributions

Conceptualization, S. K. Pradhan and M. S. Oh; Methodology, S. K. Pradhan and M. S. Oh; Validation, S. K. Pradhan and M. S. Oh; Formal Analysis, S. K. Pradhan and M. S. Oh; Writing—Original Draft Preparation, S. K. Pradhan; Writing—Review & Editing, M. S. Oh; Visualization, S. K. Pradhan and M. S. Oh.

References

[1] G. Liang, Q. Tan, Y. Liu, T. Wu, X. Yang, Z. Tian, A. Atrens, and M. X. Zhang, “Effect of cooling rate on microstructure and mechanical properties of a low-carbon low-alloy steel,” Journal of Materials Science, vol. 56, no. 5, pp. 3995-4005, 2021.

[2] S. S. Kang, A. Bolouri, and C. -G. Kang, “The effect of heat treatment on the mechanical properties of a low carbon steel (0.1%) for offshore structural application,” Proceedings of the Institution of Mechanical Engineers, Part L: Journal of Materials: Design and Applications, vol. 226, no. 3, pp. 242-251, 2012.

[3] A. Bolouri, T. -W. Kim, and C. G. Kang, “Processing of low-carbon cast steels for offshore structural applications,” Materials and Manufacturing Processes, vol. 28, no. 11, pp. 1260-1267, 2013.

[4] T. W. Yin, Y. F. Shen, N. Jia, Y. J. Li, and W. Y. Xue, “Controllable selection of martensitic variant enables concurrent enhancement of strength and ductility in a low-carbon steel,” International Journal of Plasticity, vol. 168, p. 103704, 2023.

[5] T. Inoue and R. Ueji, “Improvement of strength, toughness and ductility in ultrafine-grained low-carbon steel processed by warm bi-axial rolling,” Materials Science and Engineering: A, vol. 786, p.139415, 2020.

[6] J. Sun, C. Yang, S. Guo, X. Sun, M. Ma, S. Zhao, and Y. Liu, “A novel process to obtain lamella structured low-carbon steel with bimodal grain size distribution for potentially improving mechanical property,” Materials Science and Engineering: A, vol. 785, p. 139339, 2020.

[7] R. Ueji, N. Tsuji, Y. Minamino, and Y. Koizumi, “Ultra-grain refinement of plain low carbon steel by cold-rolling and annealing of martensite,” Acta Materialia, vol. 50, no. 16, pp. 4177-4189, 2002.

[8] A. Karmakar, M. Mandal, A. Mandal, M. B. Sk, S. Mukherjee, and D. Chakrabarti, “Effect of starting microstructure on the grain refinement in cold-rolled low-carbon steel during annealing at two different heating rates,” Metallurgical Materials Transactions A, vol. 47, no. 1, pp. 268-281, 2016.

[9] H. Mao, R. Zhang, L. Hua, and F. Yin, “Study of static recrystallization behaviors of GCr15 steel under two-pass hot compression deformation,” Journal of Materials Engineering and Performance, vol. 24, no. 2, pp. 930-935, 2015.

[10] K. K. Alaneme and E. A. Okotete, “Recrystallization mechanisms and microstructure development in emerging metallic materials: A review,” Journal of Science: Advanced Materials and Devices, vol. 4, no. 1, pp. 19-33, 2019.

[11] P. R. Rios, F. Siciliano Jr, H. R. Z. Sandim, R. L. Plaut, and A. F. Padilha, “Nucleation and growth during recrystallization,” Materials Research, vol. 8, no. 3, pp. 225-238, 2005.

[12] Y. Lü, D. A. Molodov, and G. Gottstein, “Recrystallization kinetics and microstructure evolution during annealing of a cold-rolled Fe–Mn–C alloy,” Acta Materialia, vol. 59, no. 8, pp. 3229-3243, 2011.

[13] M. Ferry, D. Muljono, and D. P. Dunne, “Recrystallization kinetics of low and ultra low carbon steels during high-rate annealing,” ISIJ International, vol. 41, no. 9, pp. 1053-1060, 2001.

[14] A. Martınez-de-Guerenu, F. Arizti, M. Díaz-Fuentes, and I. Gutiérrez, “Recovery during annealing in a cold rolled low carbon steel. Part I: Kinetics and microstructural characterization,” Acta Materialia, vol. 52, no. 12, pp. 3657-3664, 2004.

[15] E. Akbari, K. K. Taheri, and A. K. Taheri, “The effect of prestrain temperature on kinetics of static recrystallization, microstructure evolution, and mechanical properties of low carbon steel,” Journal of Materials Engineering and Performance, vol. 27, no. 5, pp. 2049-2059, 2018.

[16] J. Tian, G. Xu, W. Liang, and Q. Yuan, “Effect of annealing on the microstructure and mechanical properties of a low-carbon steel with ultrafine grains,” Metallography, Microstructure, and Analysis, vol. 6, no. 3, pp. 233-239, 2017.

[17] M. Oyarzábal, A. Martínez-de-Guerenu, and I. Gutiérrez, “Effect of stored energy and recovery on the overall recrystallization kinetics of a cold rolled low carbon steel,” Materials Science and Engineering: A, vol. 485, no. 1-2, pp. 200-209, 2008.

[18] N. A. Raji and O. O. Oluwole, “Recrystallization kinetics and microstructure evolution of annealed cold-drawn low-carbon steel,” Journal of Crystallization Process and Technology, vol. 3, no. 4, pp. 163-169, 2013.

[19] T. Ogawa, H. Dannoshita, K. Maruoka, and K. Ushioda, “Microstructural evolution during cold rolling and subsequent annealing in low-carbon steel with different initial microstructures” Journal of Materials Engineering and Performance, vol. 26, no. 8, pp. 3821-3830, 2017.

[20] S. Dutta, A. K. Panda, A. Mitra, S. Chatterjee, and R. K. Roy, “Microstructural evolution, recovery and recrystallization kinetics of isothermally annealed ultra low carbon steel,” Materials Research Express, vol. 7, no. 1, p. 016554, 2020.

[21] J. Zhang, D. Raabe, and C. C. Tasan, “Designing duplex, ultrafine-grained Fe-Mn-Al-C steels by tuning phase transformation and recrystallization kinetics,” Acta Materialia, vol. 141, pp. 374-387, 2017.

[22] K. Jeong, S. -W. Jin, S. -G. Kang, J. -W. Park, H. -J. Jeong, S. -T. Hong, S. H. Cho, M. -J. Kim, and H. N. Han, “Athermally enhanced recrystallization kinetics of ultra-low carbon steel via electric current treatment,” Acta Materialia, vol. 232, p. 117925, 2022.